

Topographic Waves in Lake Ontario¹

G. T. CSANADY

Woods Hole Oceanographic Institution, Woods Hole, Mass. 02543

(Manuscript received 14 April 1975, in revised form 12 June 1975)

ABSTRACT

Properties of a topographic wave are calculated for an idealized shore zone model simulating the north shore of Lake Ontario. Observations at the Oshawa "coastal chain" taken during the International Field Year on the Great Lakes are then scrutinized, concentrating on three flow-reversal episodes involving deep, barotropic currents. It is shown that the observed phenomena have characteristics very similar to those of the idealized topographic wave. A legitimate interpretation of the observed 12–16 day periodicities in longshore flow within the coastal zone of Lake Ontario is that they are caused by a combination of internal Kelvin waves and topographic waves. Although the speeds of these two kinds of vorticity waves are very similar in Lake Ontario, a careful consideration of the evidence clearly shows phase separation, particularly so late in the season when reduced density differences lead to a slowing down of internal Kelvin waves.

1. Introduction

During the past decade or so there has been considerable interest among oceanographers in a mode of motion which may be described as a vorticity wave tied to the topography of the sea floor. Robinson (1964) appears to have been the first to focus attention on waves of this kind as useful conceptual models in explaining observed phenomena, notably the sea-level anomalies on the Australian coast reported by Hamon (1962). Robinson called these waves "shelf waves" and suggested that they may be excited by moving pressure disturbances. Longuet-Higgins (1968) pointed out the class-similarity of these waves to other vorticity waves, notably Rossby waves and Kelvin waves. The work of Longuet-Higgins (1968) and Rhines (1969) also demonstrated that similar topographic waves may arise in locations other than continental shelves. It seems legitimate to call all such waves topographic waves, and to regard them a third member of the class of vorticity waves, to which also Rossby waves and Kelvin waves belong (as well as hybrid forms of those three).

Adams and Buchwald (1969) have shown that the important forcing mechanism in generating topographic waves along the coasts of continents is the *wind stress* acting on the sea surface (not the atmospheric pressure gradient). When acting on water of variable depth, the horizontal acceleration produced by the wind stress is inversely proportional to depth, and the nonuniformity of this generates an initial vorticity distribution. Gill and Schumann (1974) have given a general method for calculating how this distribution propagates along a

straight, infinite coast as a series of topographic waves. Important contributions to the topic are also due to Mysak (1967, 1968).

The conceptual model of a topographic wave is also easily applied to a closed basin and suggests that its interesting characteristics might be observable in large lakes, such as Lake Ontario. In a reply to a discussion by Simons (1974) I have applied such ideas to speculations concerning the effects of the earth's rotation on depth-integrated lake circulation. Simons (1975) has subsequently calculated numerically the evolution of what appears to be a topographic wave in Lake Ontario following a wind-stress impulse. The mechanics of the generation and progress of this type of wave is most concisely described in terms of vorticity arguments as follows.

As wind blows over the surface of a closed, variable-depth basin, it accelerates the shallower waters more strongly than the deep, and thereby generates vertical vorticity. The immediate effect of this is the production of closed circulation loops in the basin, which may be called "topographic gyres" (Csanady, 1975). Such gyres, once excited, would remain stationary, unchanged in pattern but decaying in amplitude in a stationary basin, but not in a rotating one. The vorticity in a topographic gyre induces flow across depth contours, which results in a stretching or squashing of vortex lines, the well-known consequence of which in a rotating system is further vorticity production. It is not difficult to show then that the net outcome of this further vorticity production is a cyclonic propagation of the flow pattern around the basin.

The whole process is very similar to the generation and propagation of Rossby waves consequent upon a

¹ Woods Hole Oceanographic Institution Contribution No. 3543.

wind-stress curl impulse over the surface of a constant depth ocean (Lighthill, 1969) or to the generation and propagation of Kelvin waves along a straight coast. In all these cases an initial impulsively generated vorticity distribution induces flow which leads to further vorticity generation and creates a "vorticity wave." In the case of Rossby waves, the flow-induced vorticity generation is due to the variation of Coriolis parameter with latitude. In the case of Kelvin waves the induced flow raises or lowers the surface level along a coast: the consequent vortex stretching or squashing provides the vorticity generation mechanism. The topographic wave is perhaps the simplest of all three, the depth variation in the path of the induced flow being the most direct possible cause of vortex stretching or squashing.

Although the vorticity arguments given above provide good intuitive ideas for the understanding of topographic waves, it is possible to explain the existence of such waves in yet simpler terms. It was pointed out above that a wind-stress impulse along the longer axis of a lake such as Lake Ontario creates topographic gyres consisting of fast longshore currents on both sides, with slow return flow in the deep water, forming a typical "double gyre" pattern. The Coriolis force acting on the two longshore jets causes a slight elevation drop on the left-hand shore (looking alongwind) and a slight rise on the right. Thus within a few hours of the application of the wind, a surface elevation gradient appears at the ends of the basin, causing water to flow around the ends. Added to the primary flow pattern, this extra flow moves the stagnation point alongshore in a cyclonic sense. Continued action of the Coriolis force on the flow on both sides of the stagnation point keeps generating a longshore pressure gradient which causes cyclonic movement of the stagnation points and with them of the entire double-gyre flow pattern.

Lake Ontario is too small to allow the development of Rossby waves, or even Kelvin waves in the barotropic mode. However, internal Kelvin waves do occur there (in the sense that flow phenomena have been observed in it with characteristics very similar to the idealized conceptual model which a Kelvin wave is). In an earlier paper (Csanady and Scott, 1974; to be referred to hereafter as CS) we have argued that certain wavelike phenomena observed nearshore during the International Field Year on the Great Lakes (IFYGL) can be interpreted as internal Kelvin waves. However, as Simons (1975) points out, similar wave-like properties also show up in the barotropic response during the very same observed episodes. Because there is no doubt about the presence of the internal Kelvin wave, one is led to the somewhat improbable conclusion that the Kelvin wave is accompanied by a topographic wave travelling at more or less the same speed. I will try to show below, by reexamining the evidence of the epi-

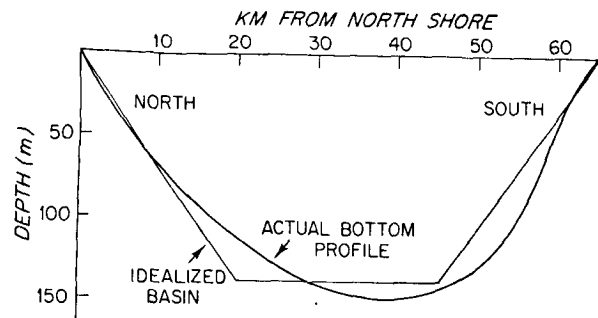


FIG. 1. Actual and idealized depth distribution in Lake Ontario along Oshawa-Olcott cross section. Note the close correspondence at the north shore to about 12 km from shore.

sodes reported in CS, that this is in fact a valid interpretation of the facts.

The internal Kelvin wave speed is proportional to the square root of the density defect, so that it is subject to at least some seasonal variation. Late in the season specifically, it should become significantly slower than earlier. This then should provide an opportunity to observe the phase separation of the topographic and internal Kelvin waves. The very last reasonably well documented wind stress episode along the IFYGL coastal chains (6-13 October 1972) does in fact show conclusively the arrival of a topographic wave at Oshawa without an accompanying Kelvin wave. The properties of this topographic wave agree with inferences one may make from a simple analytical model discussed by Mysak (1968), and the mechanism of its excitation as described by Adams and Buchwald (1969) and Gill and Schumann (1974).

2. Properties of topographic waves

A first approximation to the flow structure in a topographic wave may be obtained by appeal to an idealized model, such as the lake cross section shown in Fig. 1. The center (constant depth) portion plays no significant role, because all vorticity generation takes place over the sloping parts, and it should be sufficient to consider a single straight shore with a sloping beach, joined at the outer edge $x=l$ to a constant depth basin. The wave may be taken to be generated by a wind-stress impulse and to have therefore a longshore wavelength twice the lake's "effective" length. With some allowance for the shallow ends of Lake Ontario, we shall take this to be 250 km, equivalent to a wavelength of 500 km, i.e., a longshore wavenumber $k=2\pi/(500 \text{ km})$. This, quite possibly, is an overestimate: numerical solutions of the equations of motion show separate gyres to occur in the central and the eastern basins, which means that the central basin's effective wavelength is only about 350-400 km. The experimental evidence to be discussed comes from the central basin, from coastal observations carried out along the north shore. The beach width of $l=20 \text{ km}$ and the correspond-

ing slope suggested in Fig. 1 is an appropriate idealization for the north shore of the central basin. With a wavelength of 500 km the nondimensional beach width becomes

$$\lambda = kl = 0.25. \tag{1}$$

Mysak (1968) has discussed the topographic wave appropriate to this geometry and showed that the wave-form over the sloping beach is

$$\zeta(x) = \zeta_0 e^{-kx} L_\nu(2kx), \quad 0 < x < l, \tag{2}$$

where ζ is the surface elevation above equilibrium, ζ_0 the value of ζ at the shore, and L_ν a Laguerre function. At the outer edge of the beach this is joined to an exponential function of very slow further decay rate, of no specific interest here. In the different topographic wave modes (different ν) the surface elevations and longshore velocities, which constitute the observable properties of the wave, become insignificant beyond the edge of the beach.

The order number ν of the Laguerre function is found by solving the dispersion relationship given by Mysak. For the specific range of parameter-space which may realistically represent lakeshores (such as the depth distribution shown in Fig. 1), this dispersion relationship is nearly equal to

$$L'_\nu(2\lambda) = M(1-\nu, 2, 2\lambda) \approx 0, \tag{3}$$

where $\lambda = kl$ and M is Kummer's function (Abramowitz and Stegun, 1964). Also, for the low-frequency topographic waves, the frequency σ is approximately related to ν through

$$\sigma \approx \frac{f}{2\nu+1}, \tag{4}$$

where f is the inertial frequency, close to 10^{-4} s^{-1} in Lake Ontario. According to Eq. (13.7.2) of Abramowitz and Stegun, the lowest root of Eq. (3) is to a good approximation

$$\nu_1 = \frac{1.95}{\lambda}. \tag{5}$$

With $\lambda = 0.25$, this gives $\nu_1 = 7.8$ and a period $T = 2\pi/\sigma$ of very nearly 12 days. In such low-frequency motions the longshore velocity is nearly geostrophic and is given by

$$v = -\frac{g}{f} \frac{\partial \zeta}{\partial x}. \tag{6}$$

The maximum value of this occurs at the shore and may be found by calculating the derivative of ζ :

$$v_0 = -\frac{gk}{\sigma} \zeta_0. \tag{7}$$

With $\zeta_0 = 1 \text{ cm}$ we find approximately $v_0 = -20 \text{ cm s}^{-1}$, the negative sign signifying a velocity leaving the

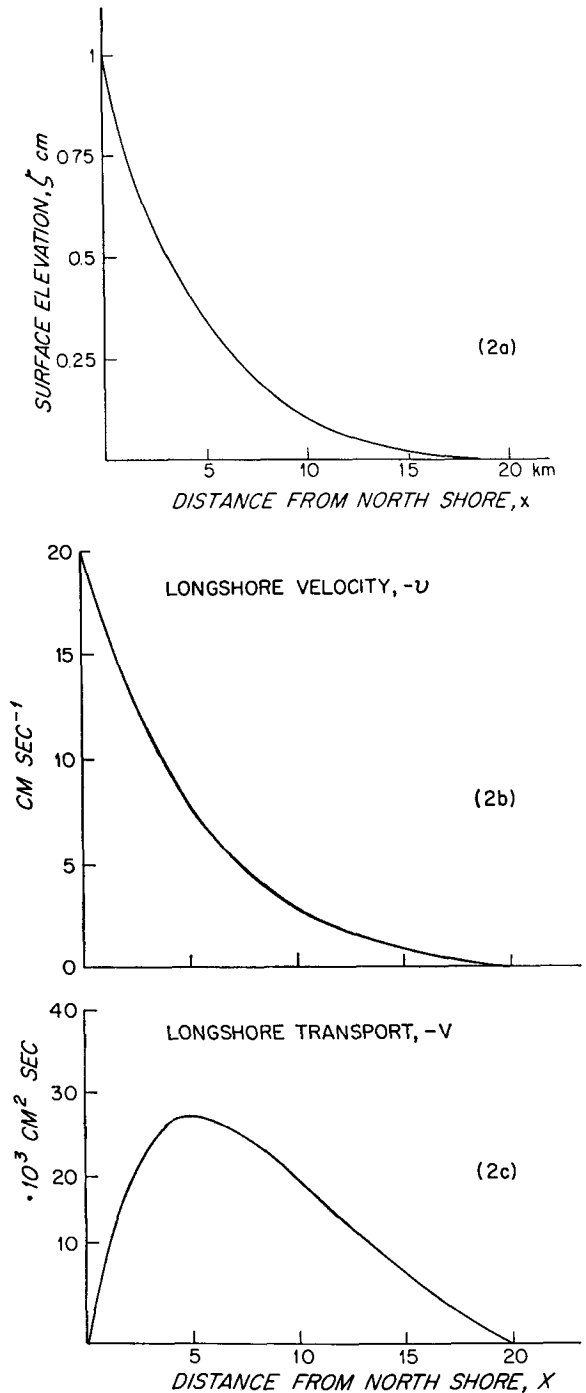


FIG. 2. Properties of topographic wave along north shore of idealized basin: (a) surface elevation, (b) longshore velocity, (c) depth-integrated transport, all for an arbitrary shore elevation amplitude of 1 cm.

shore to the right (for positive ζ_0). This reduces monotonically to zero at the edge of the sloping beach, to a good approximation. Fig. 2 shows the distribution of surface elevation, longshore velocity, and longshore depth-integrated transport over the sloping beach in

our idealized model, for the lowest order (i.e., fastest) topographic wave.

These illustrations demonstrate forcefully what one would suspect on general theoretical grounds, namely that the dominant "signature" of a vorticity wave resides in the velocity field. By sophisticated spectral analysis of surface level records it is possible to detect periodicities of the order of 12 days at an amplitude of 1 cm, but if current observations are available, a velocity amplitude of order 20 cm s^{-1} should show up a great deal more obviously.

On the basis of the analyses of Adams and Buchwald (1969) and Gill and Schumann (1974) we may now envisage the generation of topographic waves in Lake Ontario as follows. A wind-stress impulse sets up initially a pattern of topographic gyres (in the barotropic mode) much as discussed in Csanady (1973; see also Bennett, 1974). This pattern, however, does not remain stationary, but propagates cyclonically around the basin as a sum of topographic waves, the lowest order wave being presumably dominant. The initial velocity amplitude of the topographic gyres is of the order of a few tens of centimeters per second, hence the lowest order topographic wave excited has a similar velocity amplitude and a surface elevation amplitude of a few centimeters. As in the initial gyre, significant velocities and depth-integrated transports are confined to a near-shore band of order 10 km width. The speed of propagation of the fundamental topographic wave is a wavelength of 500 km provided by a period of order 12 days, i.e., a speed of the order of 50 cm s^{-1} . If the effective wavelength is less, say 350–400 km, the calculated period also reduces in roughly the same proportion as the wavelength, i.e., to 8–10 days, leaving the propagation velocity (nearly) unchanged.

Our calculations above have been based on a frictionless model. Very close to shore, of course, one cannot expect high velocities to survive frictional effects for long. Therefore, the longshore velocity in an observed wavelike phenomenon of characteristics similar to the fundamental topographic wave should be expected to peak some few kilometers from shore, but still over a pronounced bottom slope

Somewhat similar conclusions (in less detail) may be derived from numerical calculations of Simons (1975, his Figs. 6 and 7) who identified a cyclonically propagating double-gyre pattern as a topographic wave. The period of that wave, as best as one can determine from the calculated data, is about 10 days. Simons also states that Hamblin (1972) calculated the behavior of similar wavelike modes in an elliptical paraboloid model of Lake Ontario and came to the conclusion that their speed of propagation around the lake perimeter was close to 40 cm s^{-1} . Owing to the necessarily relatively coarse grid it is not possible to extract from Simon's calculations details comparable to our Fig. 2, but there seems to be no difficulty in reconciling the two results.

Further insight into the mechanics of the topographic wave may be gained by calculating in a very simple fashion how the longshore pressure gradients produce the cyclonic propagation of the wave. The elevations at shore develop in response to the Coriolis force, to establish geostrophic balance across the longshore jets. The width of these jets is of the order of the beach width l , so that geostrophic balance requires

$$fv_0 = O\left(g\frac{\zeta_0}{l}\right), \quad (8)$$

where v_0 is the velocity amplitude and ζ_0 the surface elevation amplitude which develops as the Coriolis force presses on the longshore jets. The longshore surface elevation gradient thus established is greatest across the stagnation point and has a magnitude $k\zeta_0$. The longshore acceleration is then $gk\zeta_0$ which accelerates the stagnant fluid to the velocity amplitude v_0 , within a period of $O(\sigma^{-1})$:

$$gk\zeta_0\sigma^{-1} = O(v_0) = O\left(g\frac{\zeta_0}{fl}\right), \quad (9)$$

having used Eq. (8). Cancelling $g\zeta_0$ on both sides we find

$$\sigma = O(fkl) = O(f\lambda). \quad (10)$$

Eqs. (4)–(7) above contain very similar results, with the magnitudes of $O(1)$ constants filled in. The period of the wave is seen to be determined by the ratio of the length scales kl , beach width divided by longshore wavelength, on account of the simple force-relationships implied by geostrophic balance and longshore acceleration.

3. Interpretation of some IFYGL observations

The above results suggest that topographic waves are most likely to be detectable by velocity observations in a coastal boundary layer (CBL) of some 10 km width. During the IFYGL deliberate efforts were made to observe the flow structure in the CBL, and specifically to detect coastal jets and baroclinic Kelvin waves in this region. For this reason five "coastal chains" were kept in operation during three "alert" periods, as already described (e.g., by Csanady and Scott, 1974). The details of the observational techniques were also described in that paper, as well as in some other publications referenced there.

In the CS paper, we documented the behavior of baroclinic Kelvin waves in Lake Ontario, which were excited by wind-stress impulses during July 1972. The propagation speed of these waves in midsummer is about 50 cm s^{-1} . Attention was focussed in the CS paper on the baroclinic response of the lake, partly because current data below 50 m were scant or non-existent. The depth-integrated transport (the most telling variable in the barotropic response of the lake) thus could not be estimated with full confidence. How-

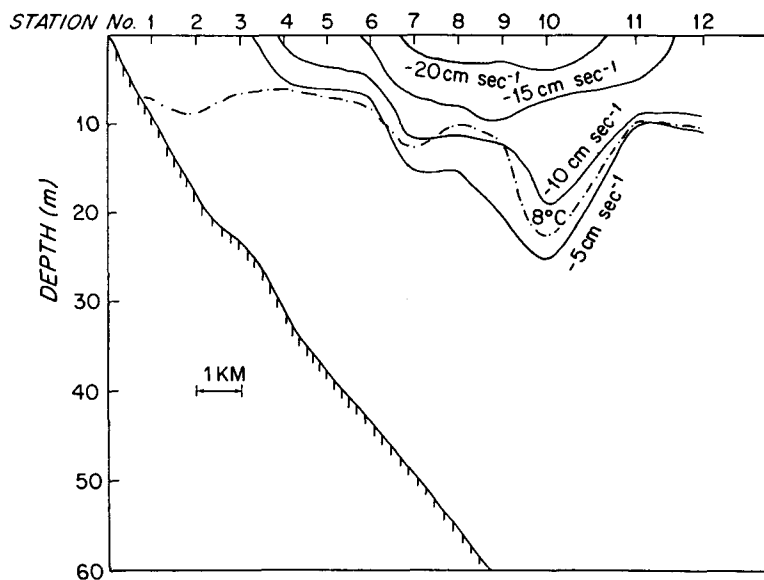


FIG. 3. Observed distribution of longshore velocity in coastal boundary layer at Oshawa, 30 July 1972. The 8°C isotherm is shown chain-dotted to indicate that significant flow is confined to the top layer.

ever, the observations extended to depths well below the thermocline and enable reasonable inferences to be made on the barotropic response, on the basis of the assumption that nothing very different occurred between 50 m and the bottom than what was observed between the thermocline and 50 m. As Simons (1975) has pointed out, inferences of this sort suggest that the nearshore *barotropic* response was also wavelike, and specifically that a barotropic wave travelled along with the internal Kelvin waves at approximately the same speed. Such a wave would therefore have to travel in a cyclonic sense around the basin at a speed close to 50 cm s^{-1} , and its effects should be most pronounced in that part of the shore zone where the coastal jets have been observed, i.e., 5–10 km from shore. As we have already seen, a topographic wave has just these characteristics and one may legitimately supplement the interpretation of data in the CS paper by the additional finding that a topographic wave apparently accompanied the internal Kelvin wave.

The fortuitous coincidence of the two wave propagation speeds has a certain *a priori* improbability and it is desirable to examine the evidence further to see if one can detect *some* difference. For this purpose the data of the Oshawa coastal chain on the north shore are especially suitable, because this was the only chain along which at least some continuous current observations were also carried out, in addition to the boat surveys (unfortunately far fewer than would have been desirable).

We first reconsider the “second episode” of CS. Strong eastward winds from 22–27 July 1972 established well-developed coastal jets at all five coastal chains,

although the eastward momentum of these on the north shore was much weaker than on the south shore, presumably on account of an offshore migration of the faster, surface waters. A wavelike reversal of the flow progressed cyclonically around the basin, which was especially noticeable during the quiescent period following the storm period, i.e., from 27 July to 1 August. This flow reversal reached Oshawa on 30 July; on the 29th only negligible velocities and a confused pattern were observed, while a well-defined westward flow appeared on the 30th. It should be emphasized that the time-integral of the wind stress over these quiescent days was low and *eastward*, so that the sudden westward acceleration had to be due to a longshore pressure gradient and the cyclonic progression of this event identifies it as a wavelike phenomenon.

The details of the flow reversal are shown in Figs. 3 and 4, negative velocities indicating westward motion. These have been replotted from the data in a somewhat different way than in CS, employing some smoothing and also showing the 8°C isotherm to illustrate the points to be made here. Clearly, the baroclinic wave arrived first in this instance, as shown by the drop of the thermocline and strong velocity differences between warm and cold layers on the 30th. These differences have more or less disappeared by the 31st, when a large deep mass of water was moving westward. The properties of this latter flow structure are very much as one would expect from the topographic wave model with the plausible rationalization of the nearshore low velocities as effects of friction. Although the coastal chain observations did not extend beyond 13–14 km from shore, the velocity magnitudes clearly decreased

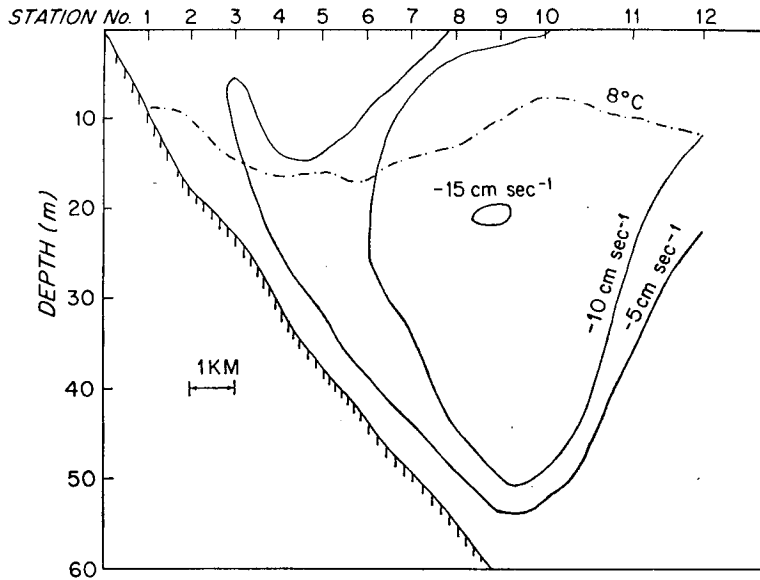


FIG. 4. Longshore velocities observed at Oshawa on 31 July 1972, with the 8°C isotherm. Note that now the bulk of longshore momentum is below the thermocline.

beyond 10 km in a manner unlikely to have been caused by friction, but pretty much as the topographic wave model predicted.

From the fixed current meter data shown in Fig. 5 it is possible to estimate a little more closely the times of arrival of the two kinds of wave. Following a quies-

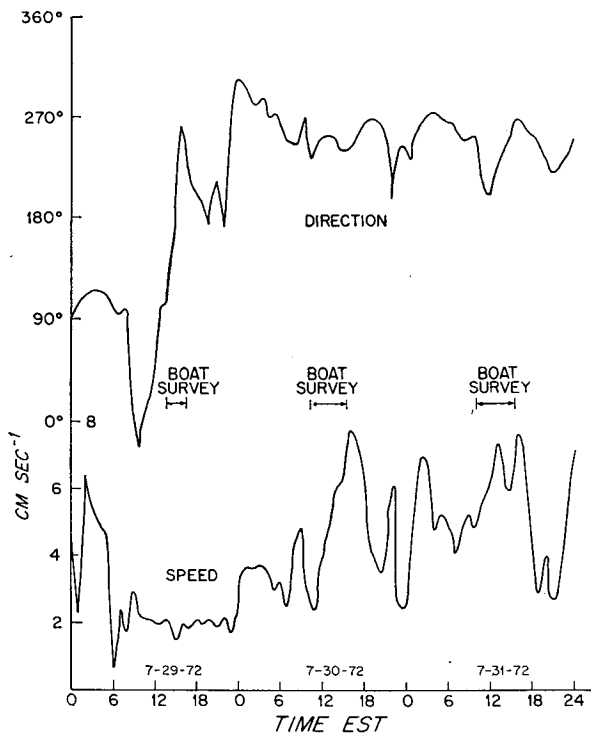


FIG. 5. Current speed and direction at 10 m depth, 1.2 km from shore at Oshawa, during 29-31 July 1972 episode.

cent period of rapid swings in current direction on 29 July, the flow turned westward and picked up some speed about midnight. This current meter was located quite close to shore, so that it is unfortunately not very easy to relate its results to the cross sections shown in Figs. 3 and 4, but it is probably correct to interpret the 3 cm s⁻¹ or so velocity early on the 30th as being that appropriate to the lower edge of the warm band, which had developed westward flow on the passage of the Kelvin wave. After about 1400 on the 30th (just when the boat survey for that day was completed) the current velocity increased noticeably to about 5 cm s⁻¹, presumably as the barotropic wave arrived. The delay time between the two waves thus seems to have been 14 h, although the current speed evidence alone is not very accurate in this regard. The comparison of the two surveys on the 30th and 31st only shows this delay to be less than 24 h.

On leafing through the original data one is struck by the difference between the uniformly low current speeds observed at Oshawa below 10 m or so all through the stormy period 22-27 July and its immediate aftermath, and the massive, deep flow on 31 July in a direction opposite to the prior strong winds. Apart from documenting the presence of a topographic wave, these data also show what a poor absorber of windward momentum the upwelled nearshore water is when the thermocline intersects the free surface some 7-10 km from shore.

The data of the first episode discussed in CS are not quite as clear-cut, partly on account of the inaccuracy of current readings on boat surveys at low current speeds. However, a deep, broad return flow also developed in this instance, at an amplitude of about 5 cm

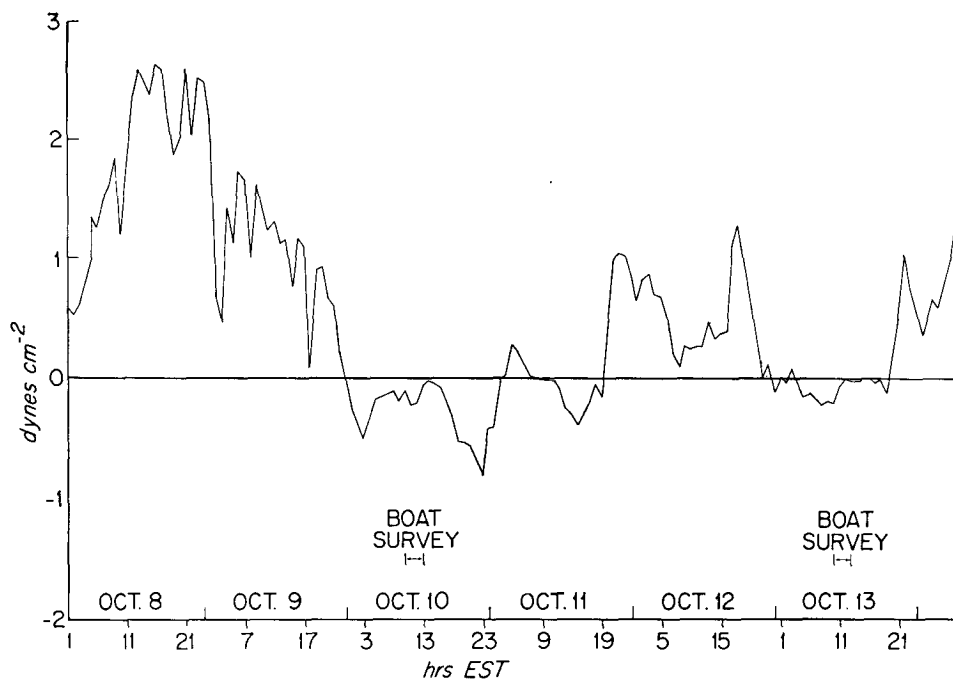


FIG. 6. East component of wind stress at buoy 6, near station 12 of Oshawa coastal chain. (Data courtesy of F. C. Elder.)

s^{-1} , on 20 July 1972, 6 days after the beginning of the stormy episode on the 14th.

The October episode has not previously been documented in the open literature.² Fig. 6 shows the history of the eastward wind stress, 8–13 October 1972. A massive impulse occurred on 8–9 October, the total at this buoy (buoy 6 located at the lakeward edge of the Oshawa coastal chain) having been about $200,000 \text{ cm}^2 \text{ s}^{-1}$ positive (eastward). This produced a thermocline upwelling and associated eastward coastal jet, as shown in Fig. 7. Near stations 9 and 10 the total eastward momentum of the water column was about $150,000 \text{ cm}^2 \text{ s}^{-1}$, i.e., close to the wind-stress input. This is in contrast to the already noted anomalous behavior of the shore zone at Oshawa during July, but similar to the July behavior of the South shore coastal chains, as discussed in CS.

The important evidence from our point of view is the boat survey presented in Fig. 8, from 13 October. A massive return (westward) flow is apparent, most markedly in the cold water below the thermocline, with peak transport in excess of $100,000 \text{ cm}^2 \text{ s}^{-1}$ about 10 km from shore. The *baroclinic* component of the flow is still eastward, its superposition having the effect of greatly reducing westward velocities above the thermocline. The eastward baroclinic flow is, as usual, accompanied by a thermocline upwelling.

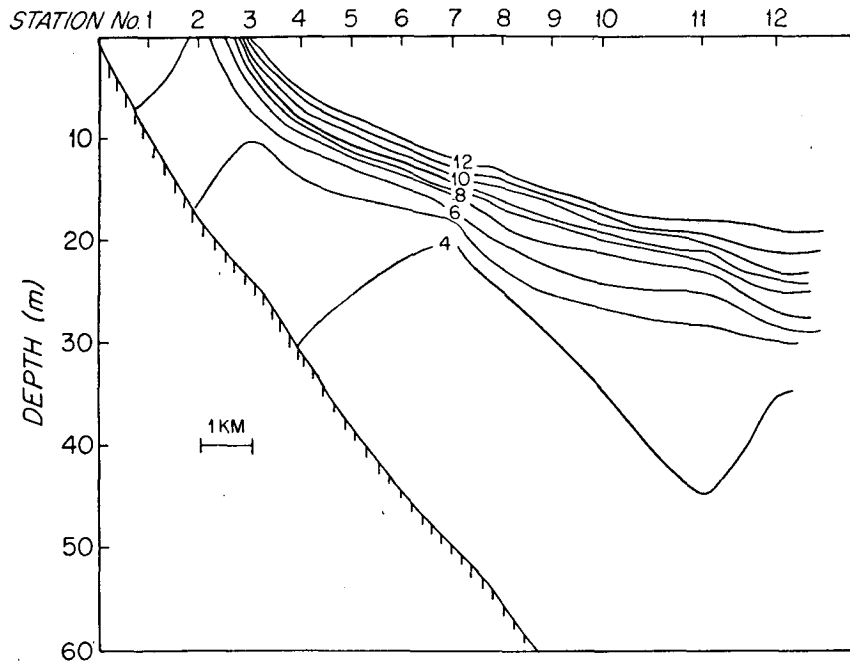
Further light is thrown on the intermediate events by the time histories of current speed, direction and

² Except for a brief reference to some current meter data by Bennett and Saylor (1974).

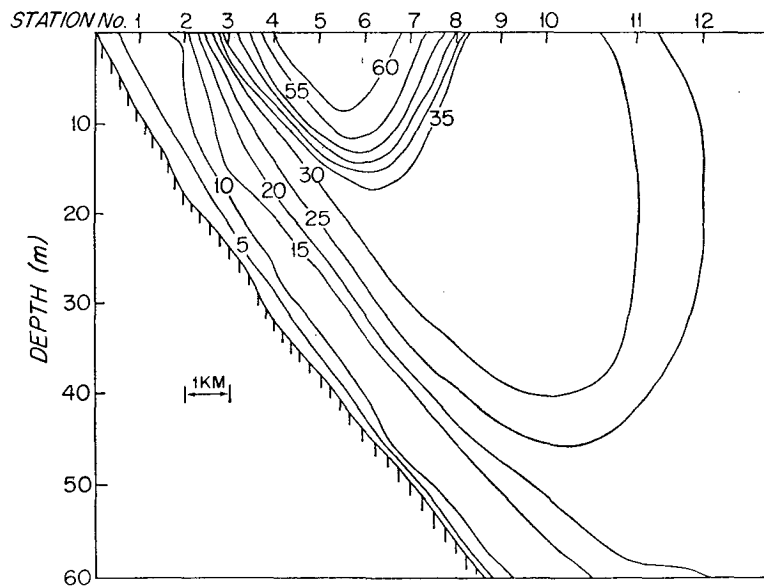
temperature at a mooring 6 km from shore, at 10 m depth (Fig. 9). The temperature record shows some thermocline oscillations following the storm, beginning with a sharp drop just prior to the boat survey on the 10th. The speed record shows the same oscillations in an even more pronounced way, the velocity gradients between warm and cold layers having been apparently stronger than temperature gradients. The direction of flow turned eastward early in the storm and remained so until a changeover period on the 12th. By early on the 13th the water was moving steadily westward at a slowly reducing speed of order 20 cm s^{-1} . The flow reversal in this instance thus appeared $4\frac{1}{2}$ days after the onset of the last major storm, rather sooner than in the July episodes, the reason for the difference being obscure. There is little doubt, however, that the pattern of flow reversal conforms to one's expectations on the basis of the topographic wave conceptual model. No internal Kelvin wave complicated this incident.

We should note here also that Blanton (1975) has examined the Oshawa current meter data systematically (the same data we have used samples of in Figs. 5 and 9 above). Blanton found pronounced periodicities of longshore flow at a period of 12–14 days. Bennett and Saylor (1974) note similar periodicities and estimate a period of 8 days. We may now legitimately ascribe such periodicities to the combined influence of two species of vorticity waves, topographic waves and internal Kelvin waves.

In further support of the topographic wave interpretation of the Oshawa flow reversals we note here some



(a)



(b)

FIG. 7. Temperature ($^{\circ}\text{C}$), a., and eastward longshore velocity (cm s^{-1}), b., distributions in a cross section along Oshawa coastal chain, on 10 October, 1972, immediately after major storm.

features of the currents observed at the Presquile coastal chain. This chain was also on the north shore, approximately 80 km to the east of Oshawa. A topographic wave should therefore appear at Presquile two days before it is observed at Oshawa. The clear-cut reversals at Oshawa were documented in the above-discussed three episodes on 20 and 30 July and 13 October. Deep, massive westward flow was indeed ob-

served at Presquile on 18 and 28 July and 11 October, all at amplitudes comparable to those observed at Oshawa two days later. The longshore velocity distribution on 11 October at Presquile is shown in Fig. 10. The temperature distribution was nearly isothermal at $8\text{--}9^{\circ}\text{C}$. The small westward wind stress impulse on 10–11 October is entirely inadequate to account for the

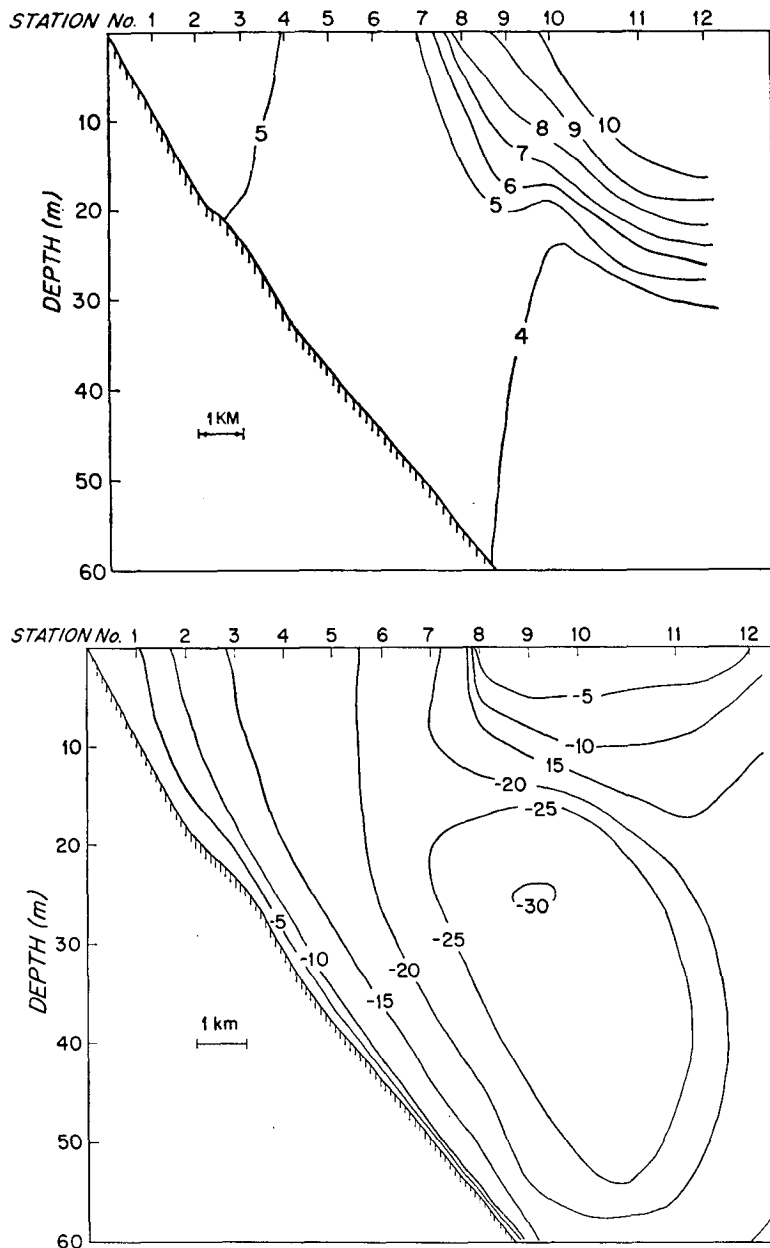


FIG. 8. As in Fig. 7 except for 13 October 1972.

westward momentum of the water ($120,000 \text{ cm s}^{-1}$ or so at Station 11).

4. Conclusion

It may be useful to restate what observed features of the three flow-reversal episodes along the north shore of Lake Ontario prompt one to invoke the topographic wave conceptual model.

1) Flow reversal appeared to propagate around the basin in a cyclonic sense at a speed close to 50 cm s^{-1} .

2) A thermocline drop and associated flow reversal confined to the warm water above the thermocline preceded the deeper flow reversal in July. A similar reversal of the baroclinic component of the flow was *not* observed in October, presumably because it lagged too far behind to be detected.

3) The barotropic flow reversal extended in all three episodes examined to a considerable water mass in the coastal zone, with depth-integrated transport peaking at 9–10 km from shore. The total reverse momentum of the water was comparable in magnitude to the

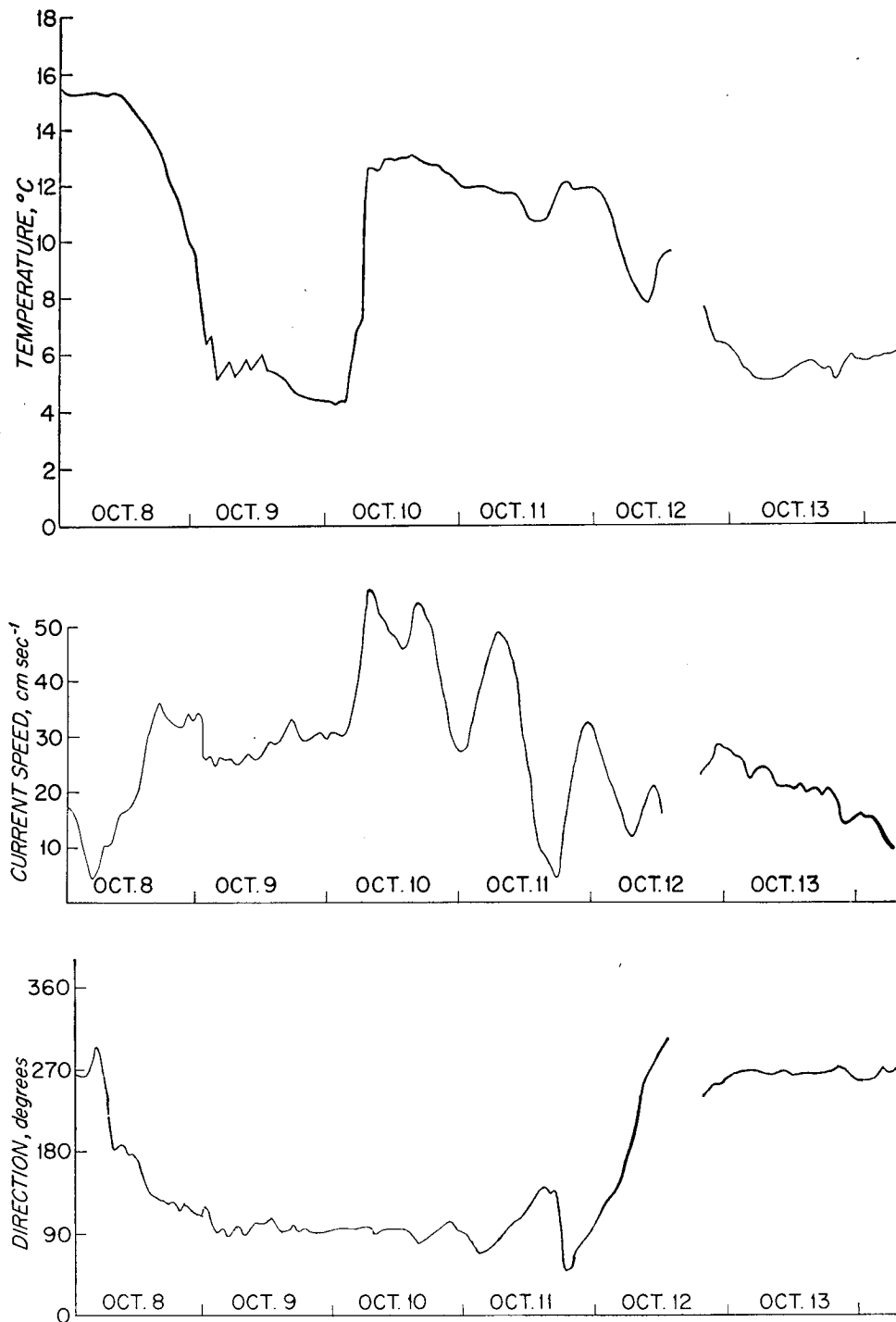


FIG. 9. Time history of temperature, current speed, and direction at fixed mooring near station 6, at 10 m depth, at Oshawa.

direct (windward) momentum input by the prior wind-stress episode which excited the event.

4) The amplitude of return flow decreased quite noticeably beyond 9–10 km, showing that the longshore

pressure gradient which produced this flow reversal decayed appreciably with distance from shore (the last coastal chain station at 13.5 km showed less than half the peak transport).

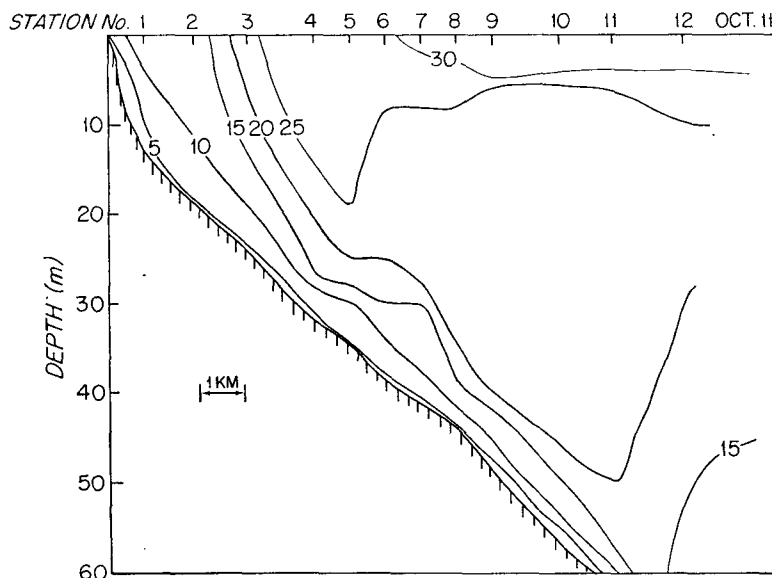


FIG. 10. Eastward longshore velocity at Presquile, 11 October 1972.

Acknowledgments. This work was supported by the Great Lakes Environmental Research Laboratory of NOAA, Ann Arbor. Wind stress values at buoy 6 were kindly placed at my disposal by F. C. Elder and moored current meter data by E. B. Bennett, both of the Canada Centre for Inland Waters.

REFERENCES

- Abramowitz, M., and I. A. Stegun, 1964: *Handbook of Mathematical Functions*. U. S. Govt. Printing Office.
- Adams, J. K., and V. T. Buchwald, 1969: The generation of continental shelf waves. *J. Fluid Mech.*, **35**, 815-826.
- Bennett, J. R., 1974: On the dynamics of wind-driven lake currents. *J. Phys. Oceanogr.*, **4**, 400-414.
- Bennett, E. B., and J. H. Saylor, 1974 IFYGL water movement program: A post field work review. *Proc. IFYGL Symp.*, 55th Annual Meeting, Amer. Geophys. Union, 102-127. Published by NOAA, Dept. of Commerce, Rockville, Md.
- Blanton, J. O., 1975: Nearshore lake currents measured during upwelling and downwelling of the thermocline in Lake Ontario. *J. Phys. Oceanogr.*, **5**, 111-124.
- Csanady, G. T., 1973: Wind-induced barotropic motions in long lakes. *J. Phys. Oceanogr.*, **3**, 429-438.
- , 1975: Hydrodynamics of large lakes. *Annual Reviews of Fluid Mechanics*, Vol. 7, 357-386.
- , and J. T. Scott, 1974: Baroclinic coastal jets in Lake Ontario during IFYGL. *J. Phys. Oceanogr.*, **4**, 524-541.
- Gill, A. E., and E. H. Schumann, 1974: The generation of long shelf waves by the wind. *J. Phys. Oceanogr.*, **4**, 83-90.
- Hamblin, P. F., 1972: Some free oscillations of a rotating natural basin. Ph.D. thesis, University of Washington, 97 pp.
- Hamon, B. V., 1962: The spectrums of mean sea level at Sydney, Coff's Harbour and Lord Howe Island. *J. Geophys. Res.*, **67**, 5147-5155.
- Lighthill, M. J., 1969: Dynamic response of the Indian Ocean to onset of the southwest monsoon. *Phil. Trans. Roy. Soc. London*, **A265**, 45-92.
- Longuet-Higgins, M. S., 1968: Double Kelvin waves with continuous depth profiles. *J. Fluid Mech.*, **34**, 49-80.
- Mysak, L. A., 1967: On the theory of continental shelf waves. *J. Marine Res.*, **25**, 205-227.
- , 1968: Edge waves on a gently sloping continental shelf of finite width. *J. Marine Res.*, **26**, 24-33.
- Rhines, P. B., 1969: Slow oscillations in an ocean of varying depth. *J. Fluid Mech.*, **37**, 161-205.
- Robinson, A. R., 1964: Continental shelf waves and the response of sea level to weather systems. *J. Geophys. Res.*, **69**, 367-368.
- Simons, T. J., 1974: Verification of numerical models of Lake Ontario: Part I. Circulation in spring and early summer. *J. Phys. Oceanogr.*, **4**, 507-523.
- , 1975: Verification of numerical models of Lake Ontario. II. Stratified circulations and temperature changes. *J. Phys. Oceanogr.*, **5**, 98-110.